Can the status of pelagic shark populations be determined using simple fishery indicators?

Felipe Carvalho[1]*, Hui Hua Lee[2], Kevin R. Piner[2], Shelley C. Clarke[3], and Maia Kapur[1]

[1]NOAA, National Marine Fisheries Service, Pacific Islands Fisheries Science Center, Honolulu, Hawaii, USA 96816
[2]NOAA National Marine Fisheries Service, Southwest Fisheries Science Center, La Jolla Shores Dr, La Jolla, California, USA 92037
[3]Common Oceans (ABNJ) Tuna Project, Food and Agriculture Organization of the United Nations (Room F322). Viale delle Terme di Caracalla, Rome, Italy 00153

*Contact author: felipe.carvalho@nooa.gov; Phone: 1 808 725 5605

Can the status of pelagic shark populations be determined using simple fishery indicators?

Abstract

Calls to develop alternative methods of assessing the population status of pelagic shark populations have increased substantially in recent years. An interim solution has been the development of more subjective evaluation of data series (indicator-based analysis) rather than predictions from complex stock assessment models. This study determines the probability with which analysts can correctly assign the population status (i.e. whether it has been overfished) and the fishing pressure (i.e. whether overfishing is occurring) based on these fishery indicator trends alone. We simulate a variety of large pelagic shark populations under different exploitation scenarios using life history parameters, and measurable fishery indicators information (catch-per-unit of effort - CPUE; and average length - AL). Our simulation results showed that the reliability of fishery indicators for establishing population status is strongly dependent upon the length of the time series analyzed and likely unreliable for when the available data series are temporally short. These caveats are critical to the proper evaluation of population trajectories that underlie the most important conservation decisions being made for sharks today.

1. Introduction

In the past fifteen years society's concern about the status and fate of the world's pelagic shark populations has awakened and intensified. This period produced some of the first studies quantifying the scope and scale of the shark fin trade, highlighting its potential to impact low-productivity shark and ray populations (Clarke et al. 2006; Worm et al. 2013). At the same time substantial expansion of the shark meat trade has been identified as a growing threat to depleted populations (Dent & Clarke 2015). Management responses have also surged since the mid-2000s with 27 new shark and ray species listed by the Convention on International Trade in Endangered Species (CITES), 26 new shark and ray species listed by the Convention on Migratory Species (CMS), and dozens of countries banning shark finning and/or the possession of shark fins.

As sharks have become the subject of greater research and heightened conservation concerns, attention has focused on assessing the reliability of historical data and understanding the biology of the species. More countries now require shark catches to be recorded and the taxonomic detail of these records has improved over time (FAO 2017). Our knowledge of shark growth, reproduction and spatial ecology has also markedly advanced through a burgeoning body of biological studies (Simpfendorfer et al. 2011; Ferry & Shiffman 2014). Despite the recent emphasis on collecting better fisheries data, the available data for assessing the health of many shark populations are still often deemed inadequate for traditional fisheries population dynamics methods. Such methods include biomass dynamics models, which incorporate catch and abundance information with basic, population-level parameters such as the carrying capacity. This approach typically requires some measure of fishing effort enacted on the species over time,

which is inherently difficult for bycatch or species which have not been closely monitored until recently.

Many of the quantitative methods used in fisheries science to determine population status (overfishing and overfished) rely on modelling total fishing mortalities (catches) and indices of abundance (catch rates). Formal stock assessments for pelagic tunas often include data extending back more than 50 years. With some exceptions (e.g. Clarke et al. 2013), reliable catch data for pelagic shark populations often are not available prior to the year 2000. Unlike sharks, tuna catch data generally represent total kills because tunas are valued, targeted species which are retained and sold. In contrast, many shark species are not the primary targets of the fisheries that catch them, and particularly when sharks are not marketed the recorded catches may represent only a fraction of the total fishing mortality. It is also often the case that sharks are actively avoided due to regulations prohibiting retention or crew safety (Gilman et al. 2008) and this can further bias catch rates. Adequate records of other fishery information such as size/sex composition of the catch can be even sparser. Understanding this limited fishery information is further complicated by the complex life history and spatial structure of pelagic shark populations (Mucientes et al. 2009; Groeneveld et al. 2014; Vandeperre et al. 2014; Carvalho et al. 2015).

Most of the pelagic shark stock assessments to date have relied on biomass dynamic or catch-at-age modelling methods which were developed for teleost fishes (e.g. Stock Synthesis (Methot & Wetzel 2013) and MULTIFAN-CL (Kleiber et al. 2014)). These modern statistical integrated modelling approaches represent powerful tools at the cutting edge of population dynamics, but they often cannot overcome the data quality issues (Maunder & Punt 2013) associated with shark populations. These models when applied to sharks have in some cases produced results considered by the investigators to be implausible or unreliable. This creates a dilemma regarding

whether to continue to apply the formal fisheries models to insufficient datasets or to defer further assessments until the data improve. The critical need to reliably assess the status of shark populations today suggests that neither of these options is particularly attractive.

An interim solution has been to develop statistical metrics (indicators) as an alternative to predictions from complex assessment models. Indicators such as nominal catch per unit of effort (CPUE) and average length (AL) of the catch are relatively straightforward to compute and track over time, and are already monitored in many fisheries (e.g. Clarke et al. 2013, Francis et al., 2014). CPUE is perhaps most frequently used as an indicator of population status, as it is often assumed proportional to abundance. Average length can also indicate population status because a decrease in size is expected as a population is exploited (Barot et al. 2004).

The case of the oceanic whitetip shark (*Carcharhinus longimanus*) is perhaps the most relevant example, where a comprehensive scientific review showed a consistent decline of CPUE and AL indicators for oceanic whitetip across three ocean basins (Western Atlantic, Indian, and Pacific Ocean) (Young et al. 2016). Based on this consistent decline in fishery indicators, combined with evidence of ongoing fishing pressure and the species' long generation period and slow growth to maturity, the U.S. National Marine Fisheries Service proposed to list this species as “Threatened” under the United States Endangered Species Act (ESA).

Indicator analysis is an increasingly popular alternative to formal stock assessment modeling because it is simple to use and can be calculated for short time series, though the assumed validity of such applications has not been confirmed. This paper examines the reliability of indicators for predicting population status of large pelagic sharks. We simulate a variety of large pelagic shark populations under different exploitation scenarios using life history parameters, and compute fishery indicators (CPUE and AL). We then examine the relationship between the

indicator trends, fishing pressure, and the population status to draw conclusions about the utility of these indicators for management.

2. Material and methods

When using fishery indicators to determine population status, the trends of CPUE and AL over time are the most commonly available information. Our objective is to determine the probability with which analysts can correctly assign the population status (i.e. whether it has been overfished) and the fishing pressure (i.e. whether overfishing is occurring) based on these fishery indicator trends alone. If so, analysts should be able to read the signal from the data and provide the most critical information required for pelagic shark management despite the continuing data deficiencies that hamper more complex assessment techniques. Here, we simulated 20,000 synthetic populations to evaluate trends of time series of CPUE and AL for prediction of population status. Our analyses involved the following steps (Fig. 1):

1) synthetic populations were simulated using a variety of pelagic shark life history information and exploitation histories over a 60-year time period;
2) the population status of each simulated population was classified based on a 2x2 contingency table representing combinations of overfishing and overfished (based on the "Kobe" plot of fisheries management);
3) a time series of fishery indicators (i.e. CPUE and AL) was calculated for each fishery;
4) the relationship between the direction of fishery indicator trends and population status was evaluated.

2.1. Simulation of pelagic shark populations

Simulations were developed using the fishery stock assessment model Stock Synthesis (SS, version V3.24O, Methot & Wetzel 2013) and the R statistical software environment (R Core Team, 2013). The SS modeling framework is widely-used to assess fish populations in the Pacific, Indian, and Atlantic oceans and is currently the only model offering a stock-recruitment relationship specifically designed for low-fecundity species, such as sharks (Taylor et al. 2013). In this study, SS was not used to fit any data, but only to create synthetic populations based on parameters controlling the systematic and fishery processes governing the population dynamics of pelagic sharks in the North Pacific Ocean. A summary of biological and fishery information used to parameterize the simulation models is presented in Appendix A (Tables A1 and A2).

The simulation models were age-structured with an annual time-step and the low fecundity stock recruitment relationship available in SS. The populations were simulated based on a set of key fishery and biological parameters including: magnitude of recruitment anomalies, steepness of the stock–recruitment relationship, individual growth rate, natural mortality rate, length and age of maturity, effort trajectory, magnitude of inter-annual variability in fishing effort, catchability (i.e., fishing mortality rate per unit of fishing effort), and shape of the function for the vulnerability-by-age of the fish population to capture. Annual recruitment deviations and fishing mortality were drawn from the appropriate distribution for each year of the simulation. Process error was included in the simulation model in the form of log-normally distributed annual recruitment deviations. Observation error was also applied to the deterministic catch prediction of the model, which assumed that fishing mortality rate is proportional to fishing effort and catchability coefficients were constant over time for each fishery.

Two simulation models were developed separately, with each model simulating 10,000 synthetic populations of pelagic sharks. The biological information used to parameterized one of

the simulation models was based on an SS assessment model for the North Pacific blue shark (hereafter referred as BSH) (Anonymous, 2017), and the second simulation model was based on a variety of mako shark-like life history traits (hereafter referred as SFM for shortfin mako, the most common mako shark species). Using SFM we intended to represent most pelagic shark species, which are traditionally placed on the K side of the life-history continuum defined by r/K selection theory (Musick 1999). This group is usually characterized by slow growth rates, long life spans, late maturity and production of limited offspring after long gestation periods (Hoenig & Gruber 1990). Compared to SFM, BSH are at the opposite end of the spectrum of pelagic shark life history characteristics. BSH are known to have a more productive life history strategy with faster growth and a higher number of smaller offspring when compared to other pelagic sharks.

Pelagic sharks inhabit very large geographic ranges that are likely to present complex movement and spatial distribution patterns. To improve our capacity to simulate true populations of SFM and BSH in the North Pacific Ocean, the simulation models built for this study are spatially explicit and can account for movement. Some assumptions were made in our application regarding the spatial and movement patterns. In our simulations both SFM and BSH populations were assumed to be distributed across three different areas, one area (Area 1) was considered as the recruitment settlement area and contains only juveniles, while the other two areas (Area 2 and Area 3) contained only adults (Fig. 2). In addition to spatial variation in size, it is well known that fish density is not uniformly distributed across space (e.g. Goethel et al. 2011). To account for spatial variability in population density, Area 2 was considered to have a higher relative abundance of adults than Area 3, as follows

$$A_{Area_2} = 0.75 * A_{total}$$

$$A_{Area_3} = A_{total} - A_{Area_2}$$

where A_{total} is the total number of adult individuals in the simulated populations. We incorporated a 10% random noise around the adult density on Area 2 to allow it to vary stochastically at each yearly time step.

Simulation studies have shown that including movement between sub-populations in stock assessments can substantially affect estimates of population size, fishing mortality, and recruitment (Goethel et al. 2011). Fish movement also has the potential to change the proportions–at–age in fished areas. Therefore, movement of BSH and SFM across all three areas was also included in the simulation. Age-based movement rates from Area 1 to Areas 2 and 3 were determined by the fraction of juvenile fish moving out at two reference ages, 1 and age-at-maturity. In the BSH and SFM simulation models, age-at-maturity was fixed at 4. Juvenile's movement from Area 1 to Areas 2 and 3 increased from 5% at age 1 to 99.9% at age-at-maturity. These rates were selected to indicate that virtually no fish stays in the recruitment settlement area after reaching the age-at-maturity (Fig. 3).

Movement between the two adult areas was also included in the simulations, with a medium hypothesis considered for movement rates. The medium movement rate was sampled from a normal distribution with mean at 0.3 and variance 0.02, which forces Areas 2 and 3 to retain around 70% of the adults. Movement rates at each age a were calculated as values in the (0, 1) range through the following transformation proposed by Lee et al. (2017):

$$\text{Movement rate}_{\text{a}} = e^{p_a}/(e^{p_a} + 1)$$

where p_a is the proportion of fish moving out of all areas at age, described above.

This inverse-logit transformation is the multiple-area realization of the generalized formula used by SS, in which the denominator contains the sum of the exponentiated parameters across

all areas in the model, where the parameter for movement to the source area (fish staying in the same area) is fixed at zero.

The population dynamics began in equilibrium without fishing. Catch in numbers, length compositions, and abundance indices for each fishery were recorded over a 60-year period. The fishing mortality in the simulation models was implemented through a fleet component, which included an individual fleet in each of the three areas. The fleet's selectivity varied across areas, and was set as time-invariant. The fleet in Area 1 was assumed to have an asymptotic selectivity, while in Areas 2 and 3 selectivity could be either asymptotic or dome-shaped (Fig. 4A).

The aim of simulating fleet specific selectivity was to reduce bias in the simulations due to the potential variety of fishing operations that catch pelagic sharks. A variety of mean fishing mortality trajectories were simulated using the algorithm developed by Carruthers et al. (2012). Fishing mortality increased at the start of the time series, remained constant, then increased or decreased after being harvested for 40 years (Fig. 4B).

2.2. Classification of population status

For each simulation, population status was determined by comparing the current spawning stock biomass (SSB_{final}) and fishing intensity level (F_{final}) to their maximum sustainable yield (MSY)-based reference points. The SSB_{final} was defined as spawning biomass estimated in the terminal year, while F_{final} was defined as an average of F estimates for the final three years to account for uncertainty and fluctuation of estimates of recent years. Population status was classified based on a 2x2 contingency table representing combinations of overfishing and overfished (based on the "Kobe" plot of fisheries management)". The "Kobe" plot offers a simple way to show if the population is in "good" or "bad" shape, depending where it falls in one

of four quadrants in the plot. The Kobe plot is based on a phase plot (i.e. one point per year) where F_{final}/F_{MSY} is plotted against SSB_{final}/SSB_{MSY}; quadrants are color coded i.e. green (not overfished, no overfishing), orange (not overfished, overfishing occurring), red quadrant (overfished and overfishing occurring), and yellow (overfished, not overfishing).

2.3. Calculation of fishery indicators

For each simulated population, two general categories of fishery indicators were evaluated; CPUE and AL. Catch, effort, and size-composition data were outputted annually for each fleet for constructing the fishery indicators. The catches are assumed to be measured without error. The fishing effort for fleet f during year t (E_t^f), is assumed to be related to the selected fishing mortality for fleet f and year t (F_t^f), as in $F_t^f = q * E_t^f$, where q is the catchability coefficient and assumed to be constant over time for each fleet. CPUE was then defined as the ratio between catch-in-numbers to the actual fishing effort (i.e. 1000 hooks) and assumed to have CV of 0.4 (a typical value in fisheries CPUE indices for bycatch species) for each observation. Each size-composition dataset was assumed to be a simple random sample of fish from multinomial distribution with effective sample size at 10 for simplicity. The size-composition data for fleet f during a given year t were assumed to be a simple random draw of fish from the catch-at-size for that year. The direction of the trends for each indicator in all three areas were summarized by calculating λ (lambda), which is the percent change in the predicted values between the first and last year from the regression divided by the number of years (i.e. average annual percent change). A negative (-) value of λ indicates a declining trend over time, while a positive (+) value of λ indicates an increasing trend over time. This method was applied for time series over three time-horizons: short length (over the last 10 years of the indicator time series); medium

length (last 30 years); and for the full length, 60 years, which extends to the beginning of the fishery.

2.4. Assessing the relationship between indicators and population status

In this study, we concentrated on assessing the relationship between the direction of trends (i.e. – λ and + λ) in CPUE and AL and the population status classification. To estimate the probability of matching a trend direction to a particular population status classification we first need to consider the total probability of a population status classification to occur $P(S)$, and the probability that a positive or negative (λ) trend of CPUE and AL co-occurs with a particular population status classification $P(\lambda \cap \mathrm{S})$. Here, we analyzed the trends of CPUE and AL jointly, therefore four possible combinations of trend directions can be assigned for each population status classification: $+_{\mathrm{CPUE}}$ and $+_{\mathrm{AL}}$; $+_{\mathrm{CPUE}}$ and $-_{\mathrm{AL}}$; $-_{\mathrm{CPUE}}$ and $+_{\mathrm{AL}}$; $-_{\mathrm{CPUE}}$ and $-_{\mathrm{AL}}$. Then, the conditional probability for the occurrence of a particular combination of trend direction (λ_c) given that a specific population status classification has occurred can be calculated by: $P\,(\lambda_c|\mathrm{S}) = P(\lambda_c \cap \mathrm{S})/P(\mathrm{S})$.

3. Results

The simulated populations were distributed within each population status classification within the Kobe plot. Most SFM and BSH populations were overfished with overfishing occurring (red areas, Fig. 5). The median value for $\mathrm{SSB_{final}/SSB_{MSY}}$ for SFM and BSH populations were 0.85 and 0.74, respectively, while the median value for $\mathrm{F_{final}/F_{MSY}}$ were 1.36 and 1.19 for SFM and BSH, respectively. Overall, simulated populations for SFM and BSH showed a similar declining trend in $\mathrm{SSB/SSB_{MSY}}$ overtime (Fig. 5). For each simulation model,

30,000 CPUE and AL trends were derived across all the simulated populations. Overall, the relationship between λ_{CPUE} and λ_{AL} and population status showed similar patterns across areas. To facilitate interpretation, here we show the results using fishery indicators from Area 2 alone. Area 2 includes most age classes as well as the highest abundance of individuals, which would make indicators from this area most representative of the overall trends in population size.

Figure 6 shows the conditional probability of occurrence of combinations of positive or negative λ_{CPUE} and λ_{AL} for simulated SFM populations in each one of the four quadrants of the Kobe plot. The conditional probabilities are presented across the three time horizons: full length, (60-year); medium length (most recent 30 years); and short length (most recent 10 years).

Both indicators with positive trend ($+\lambda_{CPUE} + \lambda_{AL}$) (Fig. 6A)

Simulations in which both indicators exhibited a positive trend for the full 60-year time series obtained a 0.91 and 0.09 probability of lying within the green and yellow quadrants of the Kobe plot, respectively. However, examining only medium (30-year) and short (10-year) time series reduced the probability that the indicators came from a population in the green quadrant to 0.66 and 0.37, respectively. This reduction was also accompanied by an increase from 0.02 to 0.16 in the probability that the indicators came from a population in the red quadrant.

Mixed-indicators trend 1 ($+\lambda_{CPUE} - \lambda_{AL}$) (Fig. 6B)

The first mixed-indicator scenario specified a positive trend in CPUE and negative trend in AL. The full 60-year time series exhibited probabilities of 0.39, 0.53, 0.06, and 0.02 that the indicators came from a population in the red, yellow, orange, and green quadrant, respectively. In comparison, reducing the duration of the examined time series to medium 30-year markedly

reduced the probability of being in the red quadrant (0.19), and increased the probability of being in the orange quadrant (0.18). Using short 10-year time series led to nearly equal probabilities of occurrence in the orange and green quadrants, 0.19 and 0.17, respectively. Red and yellow quadrants showed higher probabilities of occurrence, 0.26 and 0.38, respectively.

Mixed-indicators trend 2 ($-\lambda_{CPUE} + \lambda_{AL}$) (Fig. 6C)

The second mixed-indicator scenario specified a negative trend in CPUE and a positive trend in AL. Simulations examined using the full 60-year time series exhibited probabilities of 0.61, 0.10, and 0.29 of coming from a population in the red, yellow, and orange quadrant, respectively. The probability of occurrence in a given quadrant for this mixed-indicator scenario was very sensitive to the length of time series examined. For example, when using the short 10-year time series, the probability of the population coming from the green quadrant increased from zero (using the full 60-year time series) to 0.19. The short 10-year time series yielded a 0.26 probability that the indicators came from a population in the red quadrant, considerably lower than the estimated value using the full 60-year time series (0.61).

Both indicators with negative trend ($-\lambda_{CPUE} - \lambda_{AL}$) (Fig. 6D)

When both indicators trended downwards over the full 60-year time series, there were probabilities of 0.93, 0.01, and 0.06 that the indicators came from a population in the red, yellow, and orange quadrants, respectively. Similar to the previous scenarios, reducing the duration of the examined time series had a strong impact on the populations' probability of occurrence in different quadrants of the Kobe plot. In particular, the probability that the indicators came from a population in the red quadrant was lower when medium 30-year and short 10-year time series

were examined (0.63 and 0.38, respectively). The probability that the indicators came from a population in the green quadrant showed an increase from zero when examining the full 60-year time series to 0.13 when using the short 10-year time series.

BSH

The pattern of indicators and population status for BSH simulated populations was similar to SFM for all four combinations of indicator trends (Fig. 7A-D). Simulations based on the much better known life history of BSH were undertaken to provide the most robust example of the reliability of indicators, despite the fact that this species is the most productive of the pelagic shark populations and thus not representative. The higher productivity of BSH relative to the SFM can been seen in the lowered proportion of BSH simulations occurring in the red quadrant compared to the SFM simulations. Nevertheless, the general patterns described above hold for both species.

4. Discussion

This analysis shows that the reliability of fishery indicators for establishing population status is strongly dependent upon the length of the time series analyzed. This conclusion is important given the widespread reliance on indicator analysis for shark populations. Species-specific information on bycatch species, including sharks, has in many cases been collected only recently, leading to the prominence of indicator-based assessments in lieu of more data-intensive stock assessment models.

The performance of indicator-based analysis can be evaluated via the probability of incorrectly assigning the stock status. For example, if both CPUE and AL indicators are trending

positive, as represented in Fig. 3A, a manager may assume from the outset that the stock is in good condition (green quadrant on Kobe). The corollary applies for a dual-negative indicator combination (Fig. 3B), where both indicators are trending down and the manager may assume the stock to be in extremely bad condition (red quadrant on Kobe). These scenarios both represent hypotheses dictated by the indicator trend. The most egregious error occurs *in extremis*, whereby the stock is truly in extremely bad condition (red quadrant on Kobe) but the manager diagnoses it as good (green quadrant on Kobe). Based on our simulation for SFM, for example, when a manager examines a short 10-year time series of a population that exhibits dual-positive indicator trends and assumes the stock is good, he or she must heed the 16% probability that this stock is indeed in the red quadrant. However, the risk of this significant fault is reduced to zero when examining a time series that extends to the beginning of the fishery (60-year in our study). In the reverse scenario, the stock exhibits dual-negative trends and is presumed to be in extremely bad condition (red quadrant). Again, in our simulation based on SFM, using a short 10-year time series, the manager would face a 13% chance of making the faulty diagnosis of a stock near collapse, when the stock is indeed in the green quadrant.

A major reason why short indicator-based time series present higher risk of mis-diagnosis stock status when compared to the medium and full length time series is the condition of the population level at the start of the indicator series. For example, populations at very low abundance levels at the start of the 10 years of data may show a stabilized CPUE or AL at a post-decline depressed state. In such cases, the lack of a trend in the most recent ten years belies the major declines in previous, unobserved years. In contrast, populations at high abundance levels (lightly depleted) at the start of data collection may show declines in CPUE and AL over a short period of time which are nevertheless within safe levels of exploitation. It appears to be critical

to put short series into the context of the longer phase of exploitation, which is unfortunately the kind of reliable historical information that is often lacking.

Another issue is that the length of time covered by indicators should be considered not only in the context of the lifespan of the fishery, but the life history of the species. As example, BSH are among the most productive Pacific pelagic sharks and have a mean generation time (time required for a female to produce a reproductively active female offspring) of 8 years in the North Pacific (value estimated in this study). Relatively short indicator time series may span less than one full mean generation time of these long-lived species, which precludes measuring density-dependent feedback effects of juvenile survivorship that can vary between generations. In contrast, longer series (e.g. 30-year) are more likely to represent multiple generations thereby improving our understanding of population status. As makos, and indeed most pelagic sharks, have generation times exceeding that of blue sharks our results demonstrate that short indicator series may pose a higher risk of mis-diagnosis of stock status for the majority of pelagic sharks.

It is important to note that in any model the necessity of making simplified assumptions about population and fishery dynamics may inadvertently bias the results. Firstly, we assumed that key fishery processes such as selectivity and catchability were constant over time. It is generally accepted that these processes are seldom stationary (Walters & Martell 2004), and this could add variability and bias to our indicators. Secondly, our simulation approach was fortified by generating the AL and CPUE indices with a moderate sampling precision that is more typically associated with a target species like tuna. It is likely that this precision is better than that found in the data for a typical pelagic shark population. Finally, our model assumed relatively simple movement patterns, where many pelagic sharks are characterized by complex spatial and migratory processes, including segregation by sex and during distinct life history

periods (pupping, nursing, and mating) (Vandeperre et al. 2014**).** For these and other reasons, our simulation may not accurately represent the true state of nature in all situations and thus may be overly optimistic or pessimistic regarding indicators performance for certain populations.

Some of the problems with simple fishery indicators identified in this analysis could be solved by applying formal population dynamics models instead of indicator methods. Population dynamics models provide a framework to capture life history information and population dynamics theory, in addition to the information used in indicator analyses. However, in most cases stock assessment models still face the most fundamental problem for indicators, i.e. approximating the conditions of the population in the years preceding data collection. For the majority of shark stock assessments it is necessary to make an "educated guess" (e.g. in the form of Bayesian priors) about when the fishery started and what the catches were in the earliest years. In this respect most population dynamics models, despite being more comprehensive in their approach, are plagued by the same issues as indicators analysis. Part of the attraction of indicators may be that they simplistically ignore this and other data gaps and thereby avoid some of the issues that can render stock assessment models inconclusive.

Historical data on shark fishing is not likely to materialize anytime soon. Therefore, in addition to improving current data collection programs, scientists should focus on developing population dynamics models and evaluating their performance in light of the data limitations associated with shark populations. In the short-term, it is likely that indicators will continue to be used and it is important that they be interpreted with caution, particularly when the time series is short. This analysis has shown that indicators can be unreliable, but they are generally easy to compute and there is no reason not to monitor them as part of a comprehensive fisheries management program. Indicators can and should be used as triggers for more formal analyses,

such as stock assessments, and for identifying data improvement priorities. Furthermore, in urgent cases, such as the oceanic whitetip shark, it may be appropriate to consider a full suite of indicators in a weight-of-evidence approach to precautionary management.

Acknowledgements

This work was carried out using data provided by the International Scientific Committee for Tuna and Tuna-like Species in the North Pacific Ocean (ISC) and reflects information provided by the ISC Shark Working Group. The authors would like to sincerely thank Annie Yau (NOAA PIFSC) for reviewing early drafts of this manuscript.

Literature cited

Anonymous. 2017. Stock assessment and future projections of blue shark in the North Pacific Ocean. Western and Central Pacific Fisheries Commission Scientific Committee. Available from https://www.wcpfc.int/node/29523

Barot S, Heino M, O'Brien L, Dieckmann U. 2004. Estimating reaction norms for age and size at maturation when age at first reproduction is unknown. Evolutionary Ecology Research 6: 659–678.

Carruthers T.R. Walters C.J. McAllister M.K. 2012. Evaluating methods that classify fisheries stock status using only fisheries catch data. Fisheries Research 119: 66–79.

Carvalho F, Ahrens R, Murie D, Bigelow K, Aires-Da-Silva A, Maunder MN, Hazin F. 2015. Using pop-up satellite archival tags to inform selectivity in fisheries stock assessment models: a case study for the Blue Shark in the South Atlantic Ocean. ICES Journal of Marine Science 72: 1715–1730.

Clarke SC, McAllister MK, Milner-Gulland EJ, Kirkwood GP, Michielsens CGJ, Agnew DJ, Pikitch EK, Nakano H, Shivji MS. 2006. Global estimates of shark catches using trade records from commercial markets. Ecology Letters 9: 1115-1126.

Clarke SC, Harley SJ, Hoyle, S.D. & Rice, J.S. 2013. Population trends in Pacific oceanic sharks and the utility of regulations on shark finning. Conservation Biology 27: 197–209.

Dent F, Clarke SC. 2015. State of the Global Market for Shark Commodities. FAO Fisheries and Aquaculture Technical Paper No. 590. Food and Agriculture Organization of the United Nations, Rome.

FAO (Food and Agriculture Organization). 2016. FAO fishery commodities global production and trade database updated to 2013. FAO, Rome (accessed February 2017).

Ferry L, Shiffman DS. 2014. The Value of Taxon-focused Science: 30 Years of Elasmobranchs in Biological Research and Outreach. Copeia 4: 743-746.

Francis MP, Clarke SC, Grigg, LH, Hoyle SD. 2014. Indicator based analysis of the status of New Zealand blue, mako and porbeagle sharks. New Zealand Fisheries Assessment Report 2014/69. 109 p.

Gilman E, Clarke S, Brothers N, Alfaro-Shigueto J, Mandelman J, Mangel S, Petersen S. 2008. Shark interactions in pelagic longline fisheries. Marine Policy 32:1-18.

Goethel DR, Quinn II TJ, Cadrin SX. 2011. Incorporating spatial structure in stock assessment: movement modeling in marine fish population dynamics. Reviews in Fisheries Science 19:119-136.

Groeneveld JC, Cliff G, Dudley SFJ, Foulis AJ, Santos J, Wintner SP. 2014. Population structure and biology of shortfin mako, *Isurus* oxyrinchus, in the South-West Indian Ocean. Marine and Freshwater Research 65: 1045–1058.

Hoenig JM. Gruber SH. 1990. Life-history patterns in the elasmobranchs: implications or fisheries management. Pages 1-16 Pratt HL, Gruber SH, Taniuchi, T, editors. Elasmobranchs as living resources: advances in the biology, ecology, systematics, and the status of fisheries. U.S. Department of Commerce, NOAA Technical Report NMFS (National Marine Fisheries Service), Washington, D.C.

Kleiber P, Hampton J, Davies N, Hoyle SD, Fournier D. 2014. MULTIFAN-CL User's Guide. Available from: http://www.multifan-cl.org/.

Lee HH, Piner KR, Maunder MN, Taylor IG, Methot R. 2017. Evaluation of alternative modelling approaches to account for spatial effects due to age-based movement. Canadian Journal of Fisheries and Aquatic Sciences 74: 1832-1844.

Maunder MN, Punt AE. 2013. A review of integrated analysis in fisheries stock assessment. Fisheries Research 142: 61-74.

Methot RD, Wetzel CR. 2013. Stock synthesis: A biological and statistical framework for fish stock assessment and fishery management. Fisheries Research 142:86-99.

Mucientes GR, Queiroz N, Sousa LL, Tarroso P, Sims DW. 2009. Sexual segregation of pelagic sharks and the potential threat from fisheries. Biology Letters 5:156–159.

Musick JA. 1999. Ecology and conservation of long-lived marine animals. Pages 1-10 in Musick JA editor. Life in the slow lane: ecology and conservation of long-lived marine animals. American Fisheries Society Symposium 23. AFS Books, Maryland.

Simpfendorfer CA, Heupel MR, White WT, Dulvy NK. 2011. The importance of research and public opinion to conservation management of sharks and rays: a synthesis. Marine and Freshwater Research 62: 518-527.

Taylor IG. Gertseva V. Methot RD., Maunder MN. 2013. A stock- recruitment relationship based on pre-recruit survival, illustrated with application to spiny dogfish shark. Fisheries Research 142: 15–21.

Vandeperre F, Aires-da-Silva A, Fontes J, Santos M, Santos RS, Afonso P. 2014. Movements of Blue Sharks (*Prionace glauca*) across their life history. PLoS ONE 9(8): e103538.

Walters CJ, Martell SJD. 2004. Fisheries Ecology and Management. Princeton University Press, Princeton.

Worm B, Davis B, Kettemer L, Ward-Paige CA., Chapman D, Heithaus MR., Gruber SH. 2013. Global catches, exploitation rates, and rebuilding options for sharks. Marine Policy 40: 194-204.

Young CN, Carlson J, Hutchinson M, Hutt C, Kobayashi D, McCandless CT, Wraith J. 2016. Status review report: oceanic whitetip shark (*Carcharhinius longimanus*). Final Report to the National Marine Fisheries Service, Office of Protected Resources, Washington, D.C.

Figures legends

Figure 1. General design of the simulation study.

Figure 2. Schematic representation of the spatial stock dynamics assumed in the simulation analyses.

Figure 3. The 10,000 simulated SFM (left panels) and BSH (right panels) population status classification outcomes summarized using the Kobe plot colors and time series of SSB/SSB_{MSY} .

Figure 4. Age-based movement rates (i.e. % that move) between areas assumed in the simulation analyses. Solid blue line represents the median values of simulated movement rates and grey shaded area indicates the 95% CI.

Figure 5. A) Plotted lines represent examples of selectivity by age for the SFM simulated populations; B) Plotted lines represent examples of mean fishing mortality trajectories for the SFM simulated populations.

Figure 6. Conditional probability of occurrence of combinations of positive or negative λ_{CPUE} and λ_{AL} for n=10,000 simulated SFM populations in each one of the four categories shown in Kobe plots. The conditional probabilities are presented across the three time horizons: full length, 60-year; medium length, 30-year; and short length, 10-year, time series.

Figure 7. Conditional probability of occurrence of combinations of positive or negative λ_{CPUE} and λ_{AL} for n=10,000 simulated BSH populations in each one of the four quadrants of the Kobe plot. The conditional probabilities are presented across the three time horizons: full length, 60-year; medium length, 30-year; and short length, 10-year, time series.

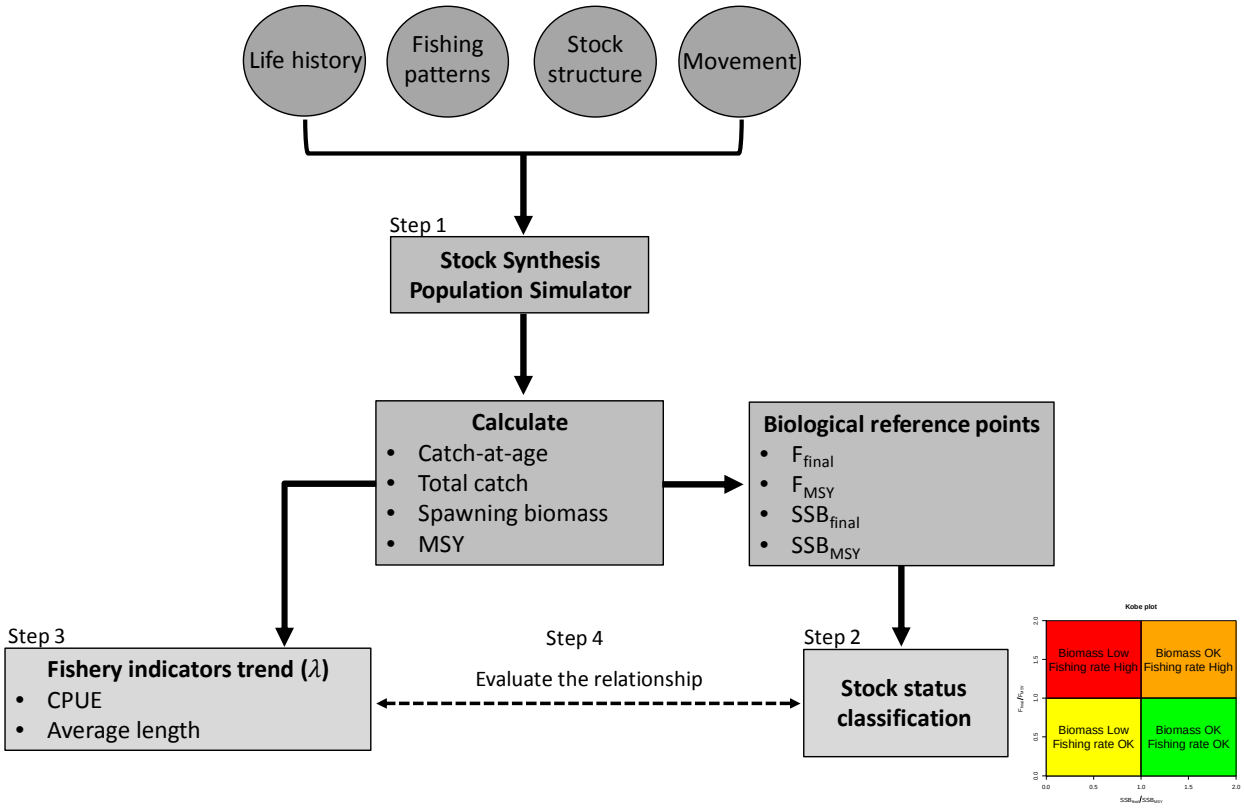

Figure 1. General design of the simulation study.

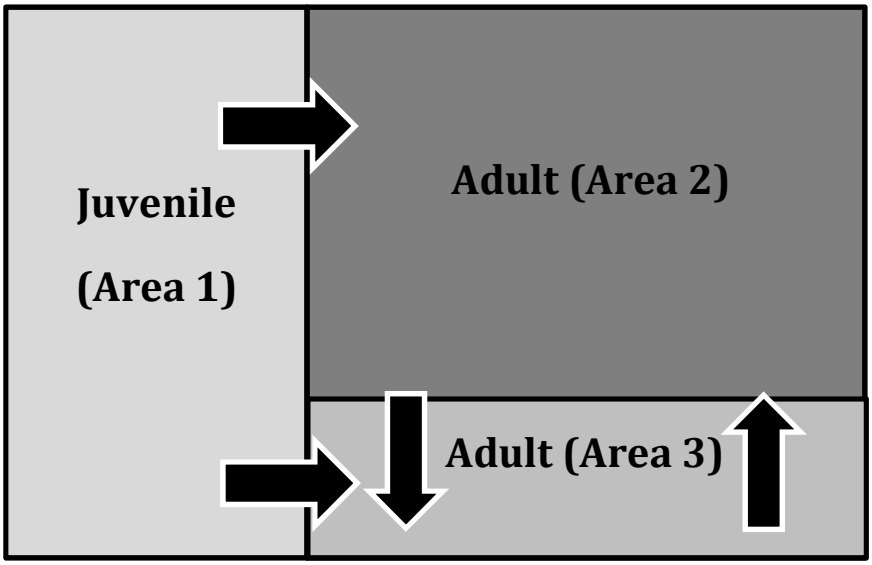

Figure 2. Schematic representation of the spatial stock dynamics assumed in this simulation analyses.

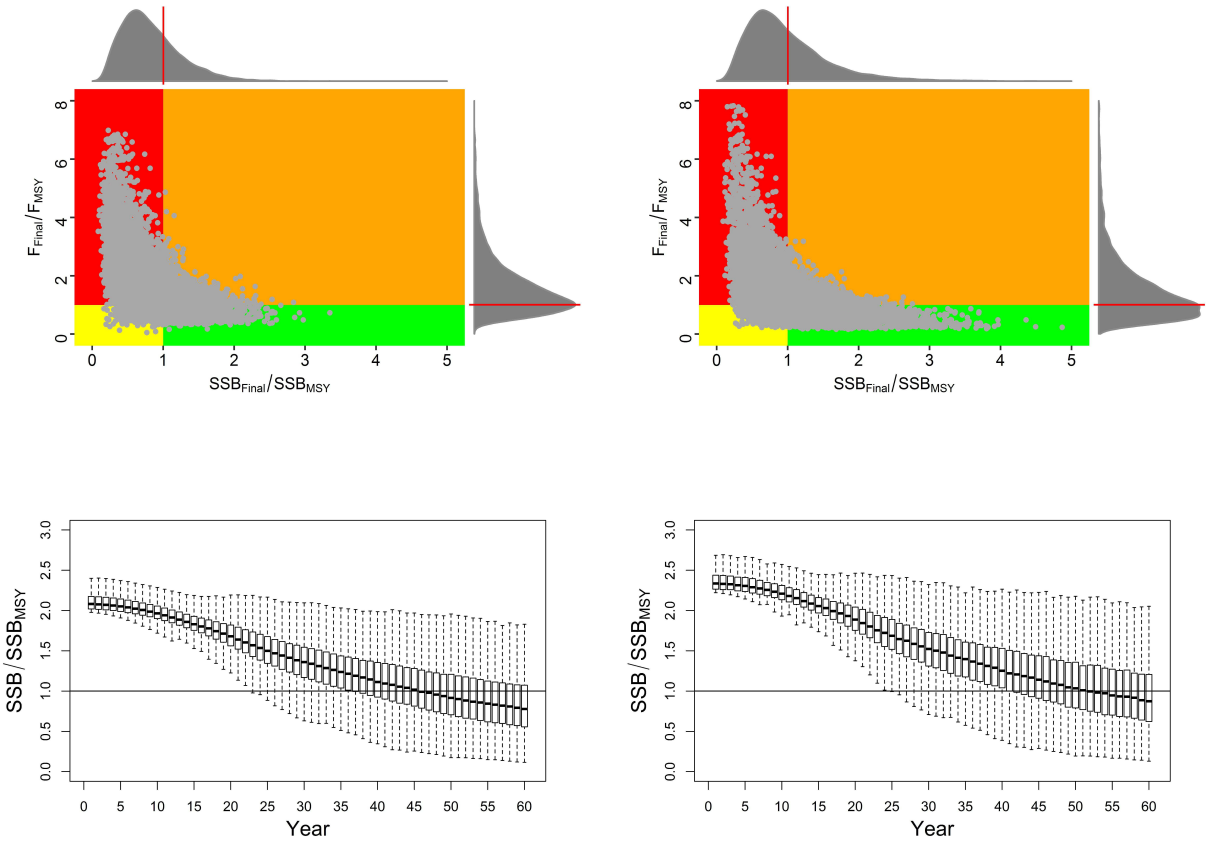

Figure 3. The 10,000 simulated SFM (left panels) and BSH (right panels) populations status classification outcomes summarized using the Kobe plot colors and time series of SSB/SSB_{MSY}.

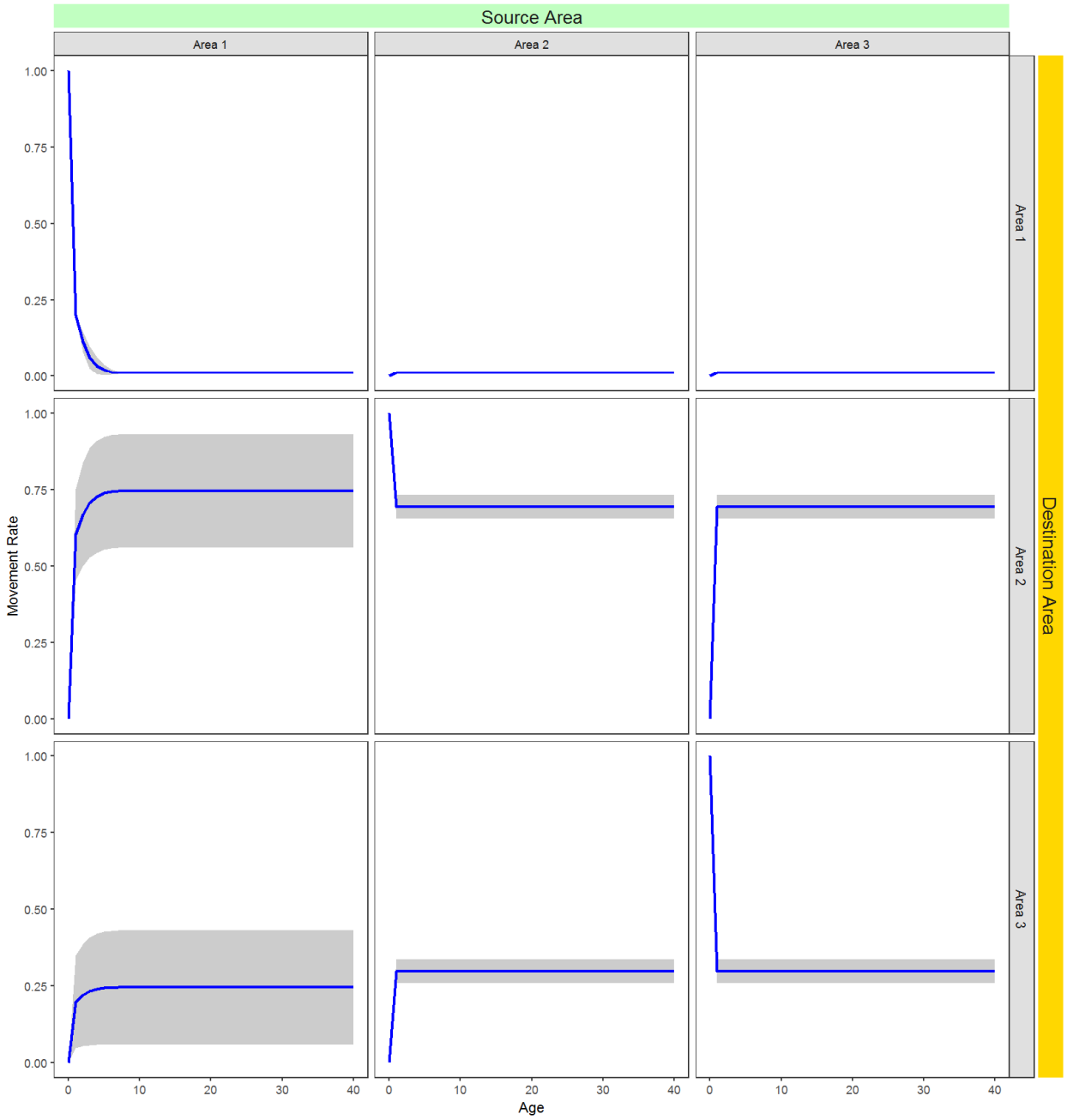

Figure 4. Age-based movement rates (i.e. % that move) between areas assumed in the simulation analyses for SFM. Solid blue line represents the median values of simulated movement rates and grey shaded area indicates the 95% CI.

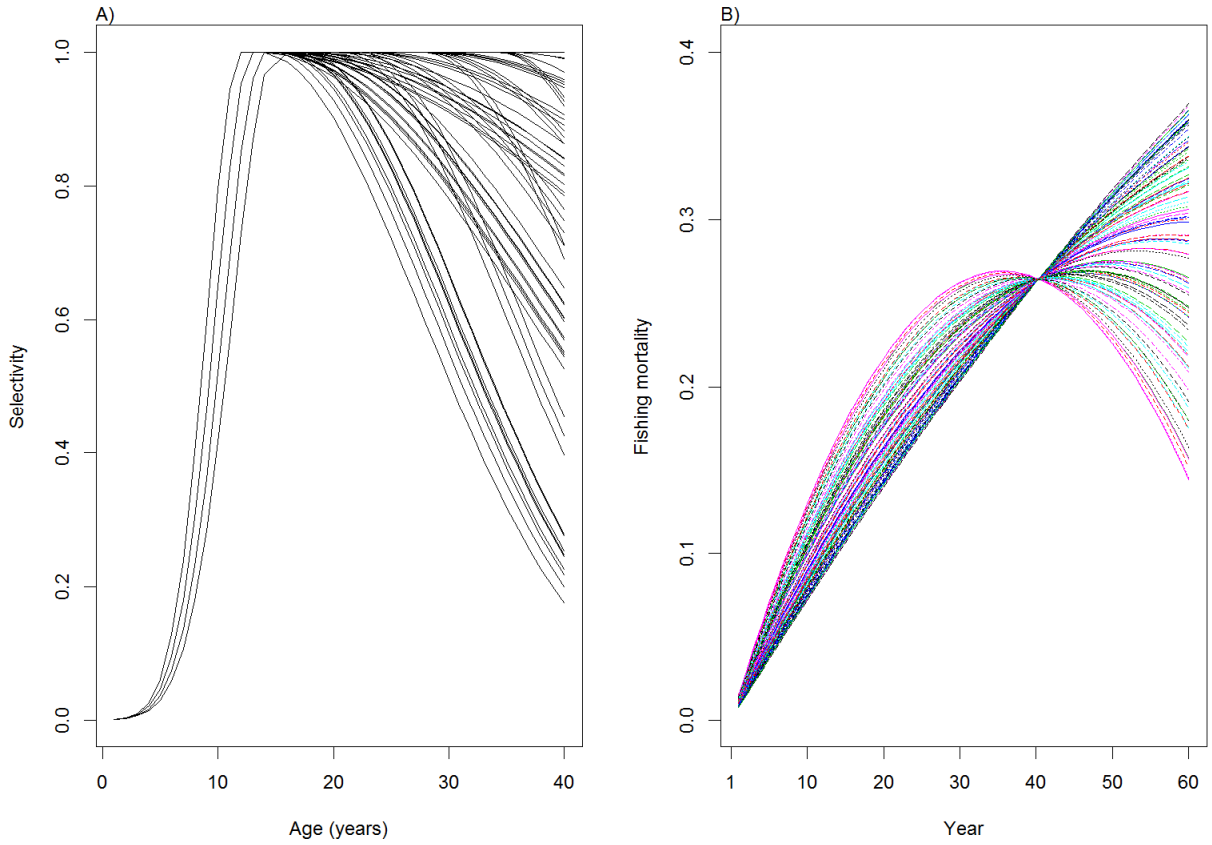

Figure 5. A) Plotted lines represent examples of selectivity by age for the SFM simulated populations; B) Plotted lines represent examples of mean fishing mortality trajectories for the SFM simulated populations.

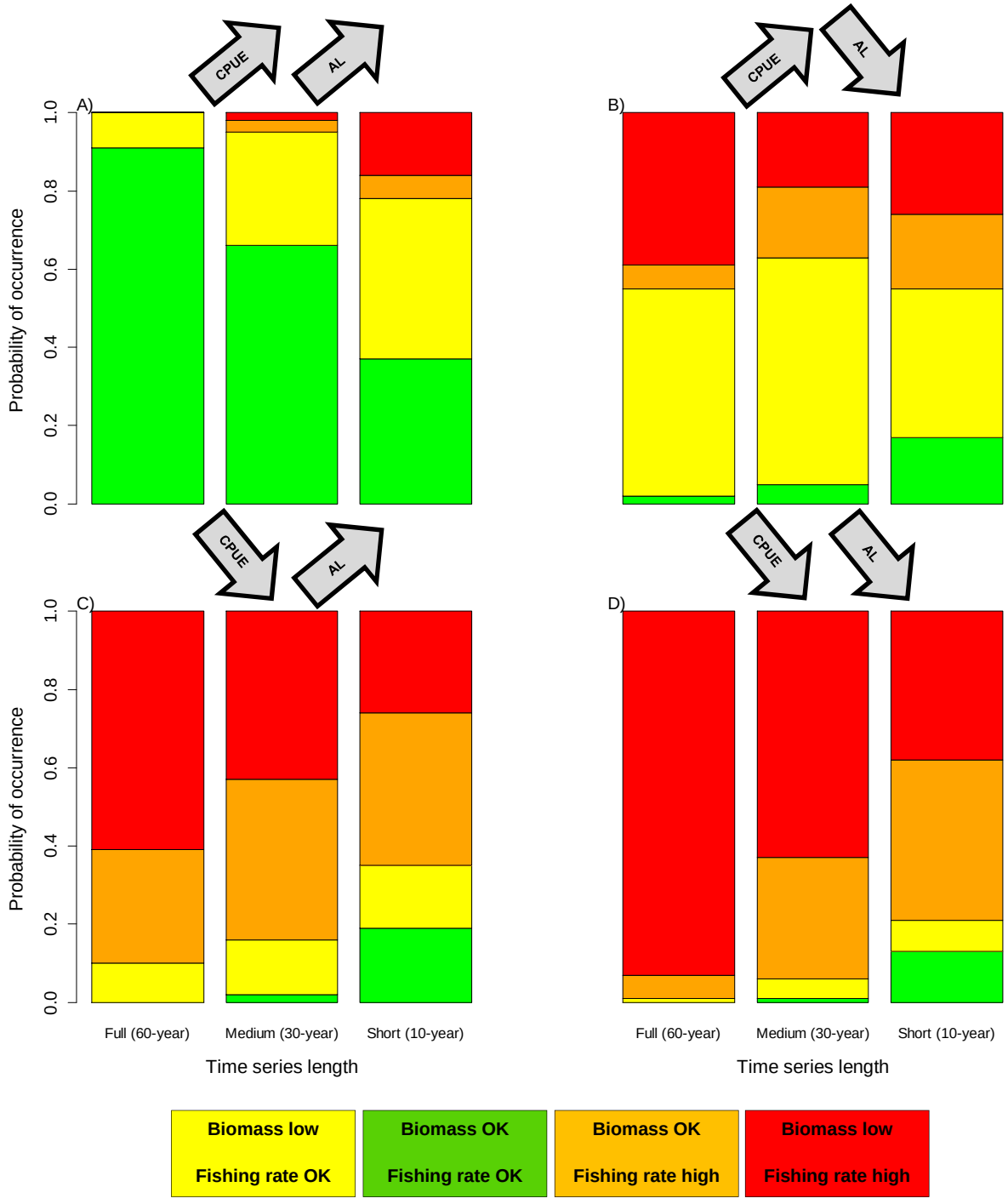

Figure 6. Conditional probability of occurrence of combinations of positive or negative λ_{CPUE} and λ_{AL} for n=10,000 simulated SFM populations in each one of the four categories shown in Kobe plots. The conditional probabilities are presented across the three time horizons: full length, 60-year; medium length, 30-year; and short length, 10-year, time series.

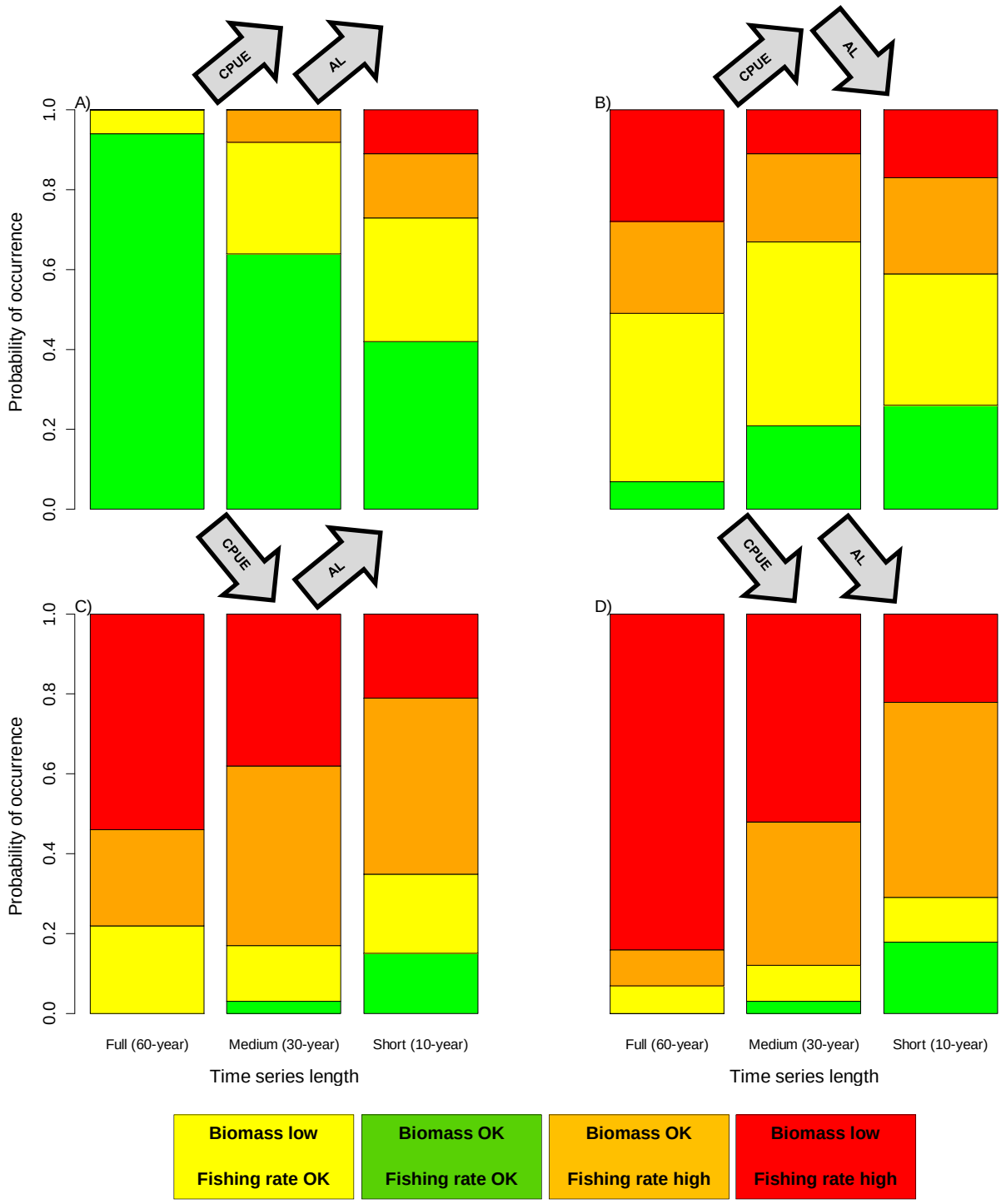

Figure 7. Conditional probability of occurrence of combinations of positive or negative λ_{CPUE} and λ_{AL} for n=10,000 simulated BSH populations in each one of the four quadrants of the Kobe plot. The conditional probabilities are presented across the three time horizons: full length, 60-year; medium length, 30-year; and short length, 10-year, time series.